Restoring Activities of Daily Living Using an EEG/EOG-Controlled Semiautonomous and Mobile Whole-Arm Exoskeleton in Chronic Stroke

Marius Nann, Francesca Cordella, Emilio Trigili, Clemente Lauretti, Marco Bravi, Sandra Miccinilli, Jose M. Catalan, Francisco J. Badesa, Simona Crea, Federica Bressi, Nicolas Garcia-Aracil, Nicola Vitiello, Loredana Zollo, and Surjo R. Soekadar

***Abstract*—Stroke survivors with chronic paralysis often have difficulties to perform various activities of daily living (ADLs), such as preparing a meal or eating and drinking independently. Recently, it was shown that a brain/neural hand exoskeleton can restore hand and finger function, but many stroke survivors suffer from motor deficits affecting their whole upper limb. Therefore, novel hybrid electroencephalography/electrooculography (EEG/EOG)-based brain/neural control paradigms were developed for guiding a whole-arm exoskeleton. It was unclear, however, whether hemiplegic stroke survivors are able to reliably use such brain/neural-controlled device. Here, we tested feasibility, safety, and user-friendliness of EEG/EOG-based brain/neural robotic control across five hemiplegic stroke survivors engaging in a drinking task that consisted of several subtasks (e.g., reaching, grasping, manipulating, and drinking). Reliability was assumed when at least 75% of subtasks were initialized within 3 s. Fluent control was assumed if average "time to initialize" each subtask ranged below 3 s. System's safety and user-friendliness were rated using Likert-scales. All chronic stroke patients were able to operate the system reliably and fluently. No undesired side effects were reported. Four participants rated the system as very user-friendly. These results show that chronic stroke survivors are capable of using an EEG/EOG-controlled semiautonomous whole-arm exoskeleton restoring ADLs.**

***Index Terms*—Activities of daily living (ADL), brain-computer interface (BCI), brain-machine interface (BMI), chronic stroke, electroencephalography (EEG), electrooculography (EOG), exoskeletons, hemiparesis, rehabilitation robotics, sensorimotor rhythms, shared control.**

I. Introduction

Stroke is one of the leading causes for long-term disability in the adulthood worldwide [1]. Besides cognitive and sensory impairments, particularly loss of hand and arm function impedes the ability of stroke survivors to engage in various activities of daily living (ADLs) such as preparing a meal or eating and drinking independently. As a consequence, stroke survivors frequently reported reduced quality of life and limited autonomy [2]. Therefore, effective restoration of hand and arm motor function after stroke is of great importance. However, there is no accepted gold standard in the treatment of stroke survivors with little or no capacity to move the arm or fingers [3], [4]. Most established rehabilitation methods such as constraint-induced movement therapy [5] require some remaining grasp function and are therefore not applicable for stroke survivors with complete hand and finger paralysis. Moreover, many stroke survivors also suffer from limited or nonexistent arm and shoulder function.

Recently, it was shown that brain/neural hand exoskeletons (B/NHEs) are capable of fully restoring hand and finger function despite complete paralysis, e.g., due to cervical spinal cord injury [6]. Such devices translate modulations of electric, magnetic, or metabolic brain activity, e.g., related to imagined or attempted movements of the paralyzed fingers, into actual finger movements driven by electromechanical actuators [7]–[10]. The best established approach for such application uses modulations of sensorimotor rhythms (SMR, 8–12 Hz) recorded by EEG

Manuscript received December 31, 2019; revised June 28, 2020 and August 28, 2020; accepted August 30, 2020. Date of publication September 17, 2020; date of current version June 16, 2021. This work was supported in part by the European Commission under the Project AIDE under Grant 645322, in part by the European Research Council under the Project NGBMI under Grant 759370, in part by the Baden-Württemberg Stiftung under Grant NEU007/1 and the Einstein Stiftung Berlin, and in part by the Italian Institute for Labour Accidents with the RehabRobo@Work under Grant CUP:C82F17000040001. The work of Surjo R. Soekadar was supported by Brain and Behavior Research Foundation as 2017 NARSAD Young Investigator Grant recipient and P&S Fund Investigator. *(Marius Nann, Francesca Cordella, Loredana Zollo, and Surjo R. Soekadar contributed equally to this work.) (Corresponding author: Surjo R. Soekadar.)*

Marius Nann and Surjo R. Soekadar are with the Charité – Universitätsmedizin, 10117 Berlin, Germany, and also with the University Hospital of Tübingen, 72076 Tübingen, Germany (e-mail: marius.nann@uni-tuebingen.de; surjo.soekadar@charite.de).

Francesca Cordella, Clemente Lauretti, Marco Bravi, Sandra Miccinilli, Federica Bressi, and Loredana Zollo are with the Università Campus Bio-Medico di Roma, 00128 Rome, Italy (e-mail: f.cordella@unicampus.it; c.lauretti@unicampus.it; m.bravi@unicampus.it; s.miccinilli@unicampus.it; f.bressi@unicampus.it; l.zollo@unicampus.it).

Emilio Trigili is with the BioRobotics Institute, Scuola Superiore Sant'Anna, 56025 Pontedera, Italy (e-mail: emilio.trigili@santannapisa.it).

Jose M. Catalan and Nicolas Garcia-Aracil are with Bioengineering Institute at Miguel Hernandez University of Elche, 03202 Alicante, Spain, and also with the New Technologies for Neurorehabilitation Laboratory, 28054 Madrid, Spain (e-mail: jcatalan@umh.es; nicolas.garcia@umh.es).

Francisco J. Badesa is with the Miguel Hernańdez University of Elche, 03202 Alicante, Spain, with the New Technologies for Neurorehabilitation Laboratory, Madrid, Spain, and also with the Universidad de Cadíz, 11003 Cádiz, Spain (e-mail: javier.badesa@uca.es).

Simona Crea and Nicola Vitiello are with the BioRobotics Institute, Scuola Superiore Sant'Anna, 56025 Pontedera, Italy, with the Department of Excellence in Robotics & AI, Scuola Superiore Sant'Anna, 56127 Pisa, Italy, and also with the IRCCS Fondazione Don Carlo Gnocchi, 50143 Florence, Italy (e-mail: simona.crea@santannapisa.it; nicola.vitiello@santannapisa.it).

Digital Object Identifier 10.1109/JSYST.2020.3021485

and quantified as SMR event-related desynchronization (SMR-ERD).

It was demonstrated that also stroke patients with cortical lesions and severe or complete finger paralysis are able to operate such brain/neural-controlled system, i.e., to drive an orthotic device opening and closing their paralyzed hands [7], [11].

While studies on upper limb motor function after stroke found that distal weakness, particular of finger movements, is more profound than shoulder and elbow weakness [12], motor compensation associated with learned nonuse, joint contractures, and pain [5], [13] may further affect whole-arm motor function.

Using an active hand exoskeleton, stroke survivors may be capable of securely grasping and holding different objects of daily living, but may remain unable to lift up and move these objects. Grasping a glass and drinking, for example, requires hand function and whole arm motor coordination for reaching and grasping a cup before guiding it to the mouth for drinking.

Therefore, we developed a novel brain/neural-controlled whole-arm exoskeleton actuating the shoulder, elbow and hand to assist in ADLs [14]. It was unclear, however, whether chronic stroke patients with upper-limb paralysis could use such brain/neural-controlled system to perform a complex task, e.g., grasping and drinking from a glass of water. The ability to perform such task would be very important, however, to broaden the scope of assistive brain/neural exoskeletons toward restoration of ADLs in everyday life environments [15].

Here, we investigated feasibility, safety, and user-friendliness of EEG/electrooculography (EOG)-based brain/neural robot control after chronic stroke to operate a vision-guided semi-autonomous whole-arm exoskeleton for restoration of ADLs.

II. Methods

The EEG/EOG-controlled semiautonomous whole-arm exoskeleton comprised the following components and control modules.

A. Whole-Arm Exoskeleton

The whole-arm exoskeleton consisted of two submodules: the newly developed shoulder-elbow exoskeleton NeuroExos Shoulder-elbow Module β (NESM β, which evolved from NESM α [16]) combined with a wrist-hand exoskeleton described in [17].

The novel second generation shoulder-elbow exoskeleton (NESM β, Fig. 1) [18] features several enhancements toward use for ADLs compared with previous versions, e.g., used in [14]. Foremost, the NESM β allows for mobile use because all elements were fully integrated into a wheelchair. Despite its compact design, essential requirements in terms of compliance, powerful actuation, and safe human-robot interaction are fulfilled. The self-aligning mechanism for improved comfort and wearability allows to follow the same passive movements of the shoulder complex as in NESM α, but integrated into a much more compact structure. The frame to fixate the shoulder-elbow exoskeleton into a wheelchair was customized and offers the possibility to have a battery-operated portable exoskeleton. Moreover, thanks to a flipping mechanism integrated in each joint allowing to manually change the arm configuration, the NESM β can mobilize the left or right upper extremity while the previous version could only mobilize the right arm and hand. The mechanical structure of the arm exoskeleton comprised four series-elastic actuation (SEA) units to realize shoulder abduction/adduction (SAA), shoulder flexion/extension (SFE), shoulder intra/extra rotation (SIE) and elbow flexion/extension (EFE). Relative to its zero-configuration with the arm laying parallel to the trunk, the four active joints allow for the following range of motions (ROMs): [0°, 85°] sA/A and sF/E, [−90°, 30°] sI/E and [10°, 100°] eF/E. Additionally, the SEA units can deliver up to 35 Nm for SAA and SFE, and up to 15 Nm for SIE and EFE.

Fig. 1. Image of the NESM β that was fully integrated into a wheelchair for mobile use. The shoulder-elbow exoskeleton can be flipped so that either the left or right upper extremity becomes mobilized.

The wrist-hand exoskeleton was composed of a 1-DOF (degree-of-freedom) wrist module that performed the activation of the pronation/supination movement, and of a 4-DOFs hand exoskeleton that allowed for flexion/extension of the thumb, index, middle and ring finger as well as pinky, simultaneously [17]. The abduction/adduction of the thumb was fixed in a predefined position.

B. EEG/EOG Control Interface

EEG was recorded from five conventional recording sites over motor cortical areas of the patient's ipsilesional hemisphere (dependent on the lesion location either F3, T3, C3, Cz, and P3, or F4, T4, C4, Cz, and P4 according to the international 10/20 system). Two additional electrodes were placed at the left and right outer canthus for EOG recordings. Reference and ground electrode were placed at FCZ and FpZ, respectively. All biosignals were sampled at 1 kHz and amplified by a wireless passive-electrode EEG system (LiveAmp, Brain Products

GmbH, Gilching, Germany). Passive polyamide-based solid-gel electrodes [19] were used to provide high wearing comfort and to make hair washing after the experimental session obsolete, a critical point to increase user-friendliness of EEG recordings in patient populations with severe paralysis.

For online processing and classification, the BCI2000 software platform was used [20]. EEG signals were first bandpass-filtered at 1–30 Hz to remove drifts and high frequency noise. Afterwards, surface Laplacian filters were applied to increase signal-to-noise ratio of the targeted electrodes at C3 or C4. Surface Laplacian filtering was shown to be very effective in allowing for specific SMR-ERD detection while suppressing signal modulations due to distant sources (e.g., eye blinks) [21]. Ipsilesional SMR-ERD during the attempt to open or close the right or left hand was calculated based on the power method by Pfurtscheller and Lopez da Silva [22]. In order to remove low-frequency drifts as well as high frequency noise, EOG signals were bandpass-filtered at 0.1–5 Hz.

C. High-Level Control Strategies

For user intention detection and control of the whole-arm exoskeleton, a shared-human robot control strategy based on a finite-state machine (FSM) was adopted. In this article, the FSM allowed the user to effectively perform the drinking task by taking the inputs from the recording devices and by controlling the whole-arm exoskeleton accordingly. In particular, the FSM controlled the transition between the subtasks as triggered by the user's biosignals [14]. In contrast to Crea *et al.* [14], there were no time constraints during activation of the interface.

A central server (based on the Yet Another Robotic Platform messaging system, YARP) managed the communication between all modules.

D. Low-Level Control Strategies

The shoulder-elbow exoskeleton motion was planned by means of a learning by demonstration (LbD) approach based on dynamic movement primitives (DMPs), with a well-defined landscape attractor [23]–[25]. This attractor allowed replicating the recorded trajectory through a weighted sum of optimally spaced Gaussian Kernels. As for a typical LbD method, trajectories performed by a demonstrator were first recorded in the joint space during the execution of ADLs by healthy subject wearing the exoskeleton (i.e., a hands-on approach was applied). Subsequently, distinctive features (called DMP parameters) were extracted using the locally weighted regression algorithm and used to train a neural network (NN) that learned the motion features and the robot's inverse kinematics. In particular, the NN was trained through the Levenberg–Marquardt supervised learning algorithm in order to associate DMP parameters and robot joint target positions to context factors taken as input (i.e., object position and task to be performed).

Thereafter, provided successful detection of the appropriate biosignal, the trained NN provided the proper set of DMP parameters and robot joint target positions for computing the set of DMPs that best fitted the desired task.

TABLE I
DEMOGRAPHIC AND CLINICAL DATA OF STROKE SURVIVORS

	P1	P2	P3	P4	P5
Age	52	49	60	39	69
Gender	M	M	M	M	F
Time from injury (yrs.)	1	6	3	5	16
Impaired limb	Right	Left	Left	Left	Left
FMA S-E-F	28	32	26	29	19
FMA W-H	17	15	9	7	16

For both the shoulder-elbow and wrist-hand exoskeletons, a position control in the joint space was adopted to drive the joint positions along a reference value or trajectory.

E. Participants

Five poststroke patients with severe hemiparesis (time since injury: 6.2 ± 5.8 years) were invited to a 2 h experimental session at the Campus Bio-Medico University of Rome, Italy. Detailed information for each stroke survivor is provided in Table I. Besides demographic data, the side of the hemiparesis as well as the upper-extremity Fugl-Meyer Assessment (FMA) score for the shoulder, elbow and forearm subsection (FMA S-E-F) and for the wrist and hand subsection (FMA W-H) are listed. While the stroke lesion in one participant affected left fronto-parieto-temporal areas, stroke lesions of the other four participants affected the right fronto-parieto-temporal areas. The lesion location was determined based on clinical magnetic resonance imaging.

All participants provided written informed consent before entering the study. The study protocol was in line with the Declaration of Helsinki and was approved by the local ethics committee (Comitato Etico Università Campus Biomedico di Roma, reference number: 01/17 PAR ComEt CBM) and by the Italian Ministry of Health (Registro - classif. DGDMF/I.5.i.m.2/2016/1096).

F. Experimental Setup, Control Paradigm, and Protocol

The study participants were comfortably seated into a wheelchair placed in front of a table where the cup was positioned (Fig. 2). Once the participants were equipped with the biosignal recording devices, EEG/EOG control signals were individually calibrated in [14]. For EOG calibration, the participants were instructed to perform five short horizontal oculoversions (HOVs) to each side. Based on the recorded EOG signals, an individual HOV detection threshold was computed. Afterwards, a SMR-ERD detection threshold was determined based on randomly presented externally paced instructions indicating either the attempt to move the paralyzed hand or to rest. For robust threshold estimation, a total of 42 trials were performed. Each calibration trial lasted 5 s with an inter trial interval of 4 s. To find an optimal SMR-ERD threshold, a

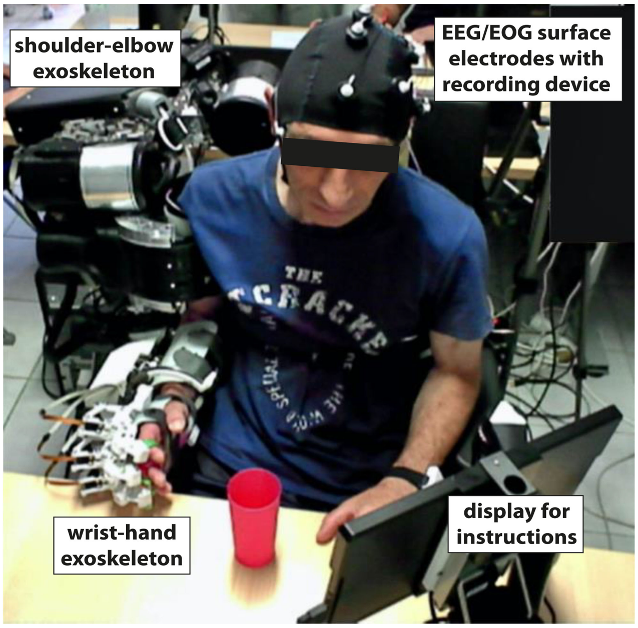

Fig. 2. Experimental setup. The hemiparetic stroke survivors were sitting in a wheelchair equipped with a whole-arm exoskeleton mounted to the patient's paretic arm and hand. EEG and EOG were recorded using surface electrodes attached to the participant's head. In order to calculate reliability and fluent control, participants received visual instructions shown on a display in front of them.

band-pass filter (± 3 Hz) was applied to the frequency showing highest SMR-ERD modulation within the SMR frequency range (8–12 Hz). The SMR-ERD threshold was then set at the two above-mentioned standard deviations the average SMR power during activation. All calibration parameters were determined at the beginning of the session and remained unaltered.

After calibration, all participants received detailed instructions about the experimental paradigm and design once more, and were familiarized with the EEG/EOG control paradigm. After familiarization, all participants were instructed to perform a total of 15 drinking tasks. Each task consisted of the following subtasks (defined by states of the FSM): i) performing HOV to trigger the shoulder-elbow unit to reach the cup. The position of the cup was *a priori* determined by an RGB-D camera; ii) continuously closing the hand exoskeleton by generating SMR-ERD exceeding the SMR-ERD detection threshold to grasp and lift the cup. Once lifted, the cup was autonomously guided to the user's mouth; iii) performing HOV to placing back the cup on the table iv) opening the hand by generating a SMR-ERD exceeding the SMR-ERD detection threshold to release the glass and go back to neutral state (Table II).

During online control within the FSM-states ii) and iv), SMR-ERD modulations were continuously translated into hand opening or closing movements as long as the SMR-ERD threshold was exceeded. Relationship between the time the SMR-ERD detection threshold was exceeded and exoskeleton movements was linear to increase the degree and intuitiveness of control (Fig. 3). This constitutes an important advancement compared to previous studies in which SMR-ERD was used as a trigger for movement initiation in [14]. A full hand exoskeleton opening

TABLE II
BMI CONTROL COMMANDS TO INITIALIZE AND EXECUTE DRINKING TASK

FSM-states	Sub-tasks of drinking	EEG/EOG control command
i.	Reaching the cup	HOV
ii.	Grasping, lifting, moving the cup to the mouth and drinking	SMR-ERD
iii.	Placing back the cup	HOV
iv.	Releasing the cup and moving back to the initial position	SMR-ERD

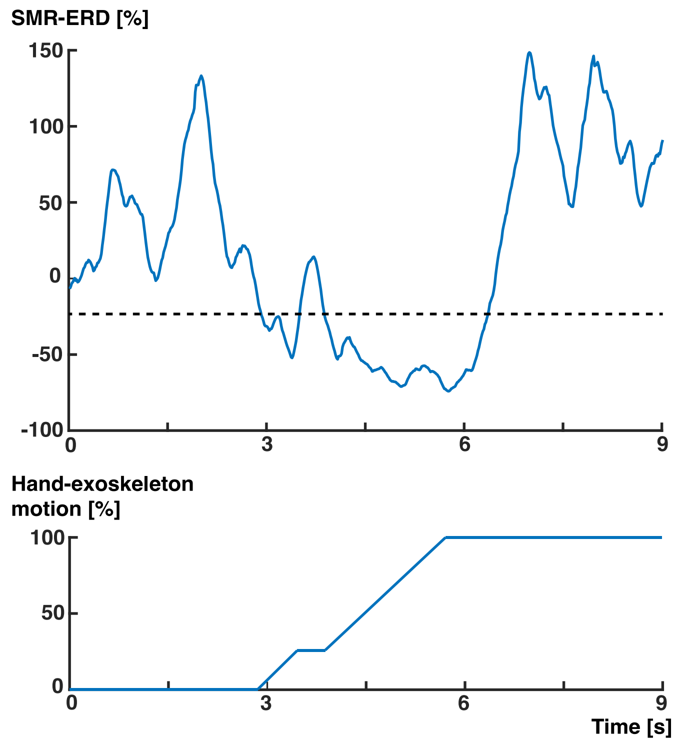

Fig. 3. Upper panel:SMR, 8–13 Hz event-related desynchronization SMR-ERD over time (blue solid line). The black dashed line represents the SMR-ERD detection threshold for hand exoskeleton opening or closing movements determined during calibration. Lower panel: Course of full hand exoskeleton closing motion related to the time the SMR-ERD detection threshold was exceeded (linear relationship).

or closing motion was achieved when the SMR-ERD detection threshold was exceeded for a time of 3 s in total.

At any given moment, participants were able to stop (veto) the ongoing action/subtask by performing HOV and reset the whole-arm exoskeleton to neutral state.

G. *Offline Data Analysis*

"Time to initialize" (TTI) each subtask was evaluated as time between visual indication to initialize the subtask and detection of the appropriate biosignal, i.e., SMR-ERD or HOV, respectively. Fluent control was assumed when average TTI ranged below 3 s [14]. Reliable control was assumed when at least 75% successful initializations were performed within 3 s. Feasibility

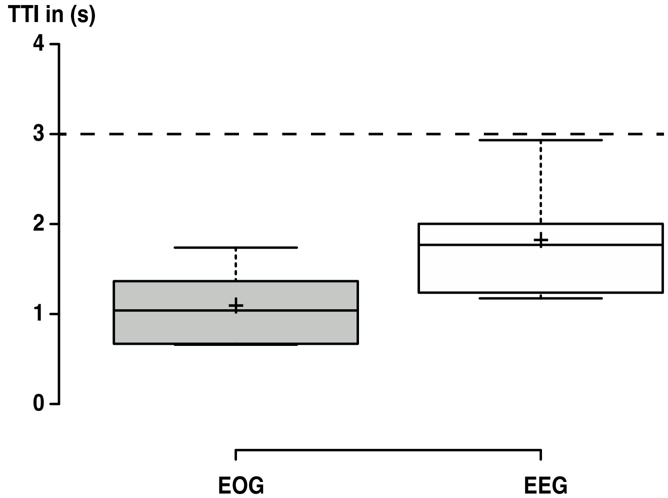

Fig. 4. TTI EOG/EOG control commands. Average TTI ranged below 3s (dashed line) documenting fluent control across both control modalities. Centerlines of boxplot show median, while crosses show the mean. Box limits indicate the 25th and 75th percentiles.

of successful EEG/EOG brain/neural robot control after chronic stroke was assumed if the criteria for reliable and fluent control were met. After the session, user-friendliness and safety aspects were assessed by a five-level Likert scale questionnaire.

III. Results

A. Feasibility

While average TTIs (±s.d.) of all EEG-controlled closing and opening hand-exoskeleton motions ranged at 1.82 ± 0.71 s (median = 1.77 s [interquartile range = 1.22–2.24 s]), EOG-controlled commands were initialized in average after 1.09 ± 0.46 s (median = 1.04 s [0.67–1.46 s]) (Fig. 4). 75% successful EEG/EOG-controlled task executions were performed within 1.88 s in average (median = 1.80 s) documenting reliable brain/neural robot control (Fig. 5 shows TTIs for each control modality). Complete hand exoskeleton closing and opening motions required in average 5.79 ± 1.18 s (median = 5.51 s [4.87–6.43 s]).

B. User-Friendliness and Safety

User-friendliness of the system was rated at 87 ± 21% of the maximum achievable score documenting a very good user experience. With 91 ± 20% of the maximum achievable score, also system safety was rated as very high by the hemiparetic participants.

Most importantly, none of the stroke survivors reported any side effects or adverse events during the use of the system (such as discomfort or pain). The preparation and mounting procedure were evaluated as comfortable and the participants reported that the calibration instructions were easy to follow. After familiarization, all participants felt safe during the drinking paradigm (Table III).

IV. Discussion

Up to one-third of all stroke survivors suffer from chronic motor deficits that impede their ability to perform ADLs [26], [27]. Driven by recent advancements in the field of wearable robotics and noninvasive neurotechnologies, brain/neural-controlled exoskeletons represent a promising tool to restore intuitive control of movements after stroke. While it was shown that EEG/EOG-based brain/neural control paradigms can be used to restore the ability to eat and drink independently after high cervical spinal cord injury [6], it remained unclear whether chronic stroke patients with severe upper-limb paralysis and different levels of chronicity (1–16 years poststroke) are capable of using such paradigm to reliably operate a semiautonomous whole-arm exoskeleton assisting in ADLs, such as grasping a cup and drinking. Thus, the primary aim of this article was to demonstrate feasibility, safety, and user-friendliness of a noninvasive brain/neural whole-arm exoskeleton for upper limb movement restoration across five chronic stroke patients engaging in a drinking task. Due to the limited bandwidth of EEG-based robotic control (typically allowing for real-time classification of up to three features only, e.g., open versus close, hand versus foot movements, or rest), the drinking task was divided into several subtasks using a FSM and coupled with a context-aware (vision-guided) actuator system. This considerably reduced the amount of necessary control signals that have to be extracted from the stroke survivor's biosignals to execute the task, essentially reducing such information for detection of the target intention and a *veto* signal.

We found that all study participants were able to operate the semiautonomous brain/neural-controlled whole-arm exoskeleton and achieved reliable and fluent control as tested during the drinking task. In average, more than 75% of successful task initializations were reached within 3 s (1.04 s for EOG and at 2.64 s for EEG) documenting reliable control, whereas the average TTI of all EEG/EOG-controlled operations ranged far below 3 reflecting fluent operation (EOG: 1.09 ± 0.46 s, EEG: 1.82 ± 0.71 s). There were no adverse effects reported and all participants felt safe to operate the system.

These results confirm that noninvasive EEG/EOG-based brain/neural robot control is a suitable strategy to restore ADLs in chronic stroke survivors with severe upper-limb motor deficits. While, in principle, EEG or EOG could be used for control of all tasks (e.g., EEG for reaching/retracting or EOG for opening/closing the hand), we reasoned that the chosen combination of EEG/EOG signals would provide a good balance between intuitiveness, reliability, and ease of use. One important rationale for the chosen combination is based on the source location and specificity of motor-related modulation of electric brain activity. Previous studies have shown that the cortical representation of finger and wrist muscles are larger and more lateralized than representations of shoulder and upper arm muscles [28]–[30]. Moreover, besides being more intuitive, EEG exoskeleton control could also trigger neural recovery [31], which makes EEG-control a potentially useful strategy in stroke neurorehabilitation [32]. However, EEG control is also more effortful and less reliable compared to EOG control. We thus

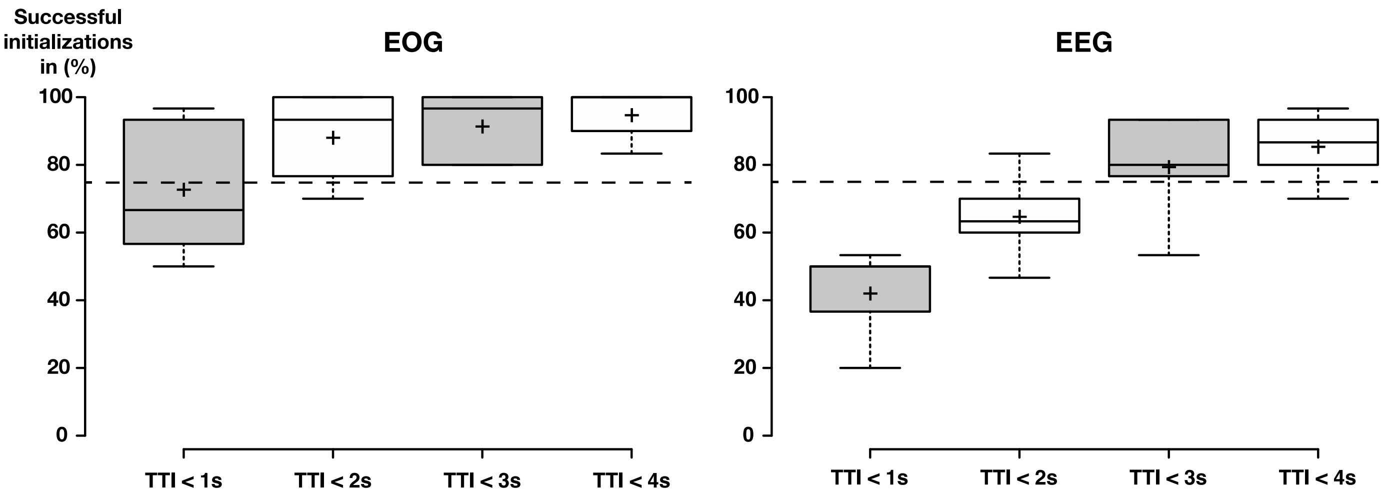

Fig. 5. Fluency of brain/neural robot control using EOG (left panel) and EEG (right panel) signals. Each boxplot summarizes the relative number of successful initializations with TTIs below discrete time intervals. Reliability was assumed when 75% of successful initializations were performed within 3s (i.e., TTI $<$ 3s, dashed line shows 75% threshold). For EOG control, the reliability criterium was met after 1.04 s in average (median = 1.16 s), while EEG control required 2.64 s in average (median = 2.56 s) to meet this criterium. Centerlines of boxplot show median, while crosses show the mean. Box limits indicate the 25th and 75th percentiles.

TABLE III
SUMMARY TABLE OF THE FIVE-LEVEL LIKERT SCALE QUESTIONNAIRE IN %. (LIKERT SCALE FROM 1 = "STRONGLY AGREE" TO 5 = "STRONGLY DISAGREE")

Likert Scale	1	2	3	4	5
I experienced side-effects or discomfort during the session	0	0	20	0	80
I felt comfortable with the whole-arm exoskeleton	20	60	20	0	0
Control of the exoskeleton was reliable and practical	60	20	0	20	0
After completing the training, I felt safe using the exoskeleton	80	20	0	0	0
The preparation/attaching process was comfortable	40	40	20	0	0
The calibration instructions were easy to follow	80	20	0	0	0
I felt discomfort/pain while electrodes/ exoskeleton were attached	0	0	0	0	100

reasoned that using EEG for hand opening/closing motions and EOG for reaching/retracting would offer the optimal balance between intuitiveness, reliability, and ease of use. Studies that further investigate the optimal control strategies depending on the purpose of brain/neural control (e.g., assistance in ADLs, neurorehabilitation, or a combination of both, [15]) will be necessary.

While all participants were able to modulate ipsilesional SMR-ERD it cannot be excluded that stroke survivors with extensive cortical lesions show limited or nonexistent ipsilesional SMR-ERD. In such case, calibration with a 64-channel high-density EEG might be necessary to identify remaining SMR modulations specifically related to movement attempts with the paralyzed hand and finger.

In our study, all participants were brain-machine interface (BMI)-naïve, i.e., they have never engaged in any brain/neural robot control before. Nonetheless, they were all able to reliably perform the drinking task shortly after calibration and familiarization. All participants stated that the calibration instructions were easy to follow. This underlines the applicability and practicality of the presented brain/neural control paradigm to operate assistive robotic devices.

While realtime classification of EEG signals does not allow to reliably differentiate different grasp-types (i.e., palmar grasp, lateral pinch, etc.) or different movement trajectories, such information can be inferred or extrapolated—to some degree—by context-aware robotics. It is important, however, that in such shared-control paradigm a reliable *veto* function is implemented that allows the user to stop unwanted behavior of the robotic device [33]. Future neurotechnologies, e.g., using quantum sensors [34], [35], may overcome the current constraint of limited spatial resolution when recording brain oscillatory activity noninvasively.

While this article paves the way for larger clinical trials, it remains to be shown how our results can be generalized to multiple sessions and to other patient populations, e.g., with traumatic brain injury, multiple sclerosis, or progressive neurodegenerative disorders, such as amyotrophic lateral sclerosis.

Given that a number of randomized clinical trials suggest that repeated use of brain-controlled exoskeletons can trigger neural recovery [36], it is conceivable that the introduced paradigm will also improve adoption of brain-controlled robotics in the context of stroke neurorehabilitation [31]. Ideally, such device should be mounted [37] and operated by the hemiplegic stroke survivor without any assistance [15]. However, to achieve this, a number of technical challenges need to be solved. For instance, the whole-arm exoskeleton is currently integrated into a wheelchair because the gears and motors do not allow for portability. While this may be acceptable for patients who are unable to walk, e.g., individuals with quadriplegia after brain stem stroke, the majority of stroke survivors are still capable of walking. Here, development of a fully portable and lightweight and modular soft-exoskeleton system [38] for the upper extremity might be a promising venue.

Another technical challenge relates to the EEG-cap. Most EEG electrodes are integrated into a textile cap that cannot be mounted without another person's assistance. Headsets using soft electrodes, e.g., based on felt or conductive polymers, that hemiplegic stroke survivors can put on unassisted are important prerequisites to broaden the applicability of brain/neural assistive systems. Here, minimizing the required recordings sites for brain/neural robot control, particularly from the face region as required for EOG recordings, would be particularly desirable [37].

Due to the heterogeneity of remaining motor functions, any strategy aiming at restoration of movement after stroke should be highly individualized and oriented toward specific individual needs [39], [40]. In this context, implementation of tools that allow for longitudinal quality-of-life assessment and tracking of the actual use of assistive systems in everyday life environments will be critical.

References

[1] G. B. D. S. Collaborators, "Global, regional, and national burden of stroke, 1990–2016: A systematic analysis for the global burden of disease study 2016," *Lancet Neurol.*, vol. 18, no. 5, pp. 439–458, May 2019, doi: 10.1016/S1474-4422(19)30034-1.

[2] W. Rosamond *et al.*, "American heart association statistics committee and stroke statistics subcommittee. Disease and stroke statistics—2008 update: A report from the american heart association statistics committee and stroke statistics subcommittee," *Circulation*, vol. 117, no. 4, pp. e25–e146, 2008.

[3] J. M. Veerbeek *et al.*, "What is the evidence for physical therapy poststroke? A systematic review and meta-analysis," (in English), *PLoS One*, vol. 9, no. 2, pp. e87987–e87987, 2014, doi: 10.1371/JOURNAL.PONE.0087987.

[4] S. M. Hatem *et al.*, "Rehabilitation of motor function after stroke: A multiple systematic review focused on techniques to stimulate upper extremity recovery," (in English), *Frontiers Human Neurosci.*, vol. 10, pp. 442–442, 2016, doi: 10.3389/FNHUM.2016.00442.

[5] E. Taub, G. Uswatte, and R. Pidikiti, "Constraint-induced movement therapy: A new family of techniques with broad application to physical rehabilitation–a clinical review," *J. Rehabil. Res. Develop.*, vol. 36, no. 3, pp. 237–251, Jul. 1999. [Online]. Available: https://www.ncbi.nlm.nih.gov/pubmed/10659807.

[6] S. R. Soekadar *et al.*, "Hybrid EEG/EOG-based brain/neural hand exoskeleton restores fully independent daily living activities after quadriplegia," *Sci. Robot.*, vol. 1, no. 1, 2016, Art. no. eaag3296. [Online]. Available: http://robotics.sciencemag.org/content/1/1/eaag3296.abstract.

[7] E. Buch *et al.*, "Think to move: A neuromagnetic brain-computer interface (BCI) system for chronic stroke," *Stroke*, vol. 39, no. 3, pp. 910–917, Mar. 2008, doi:10.1161/STROKEAHA.107.505313.

[8] S. Soekadar, N. Birbaumer, and L.G. Cohen, "Brain–computer interfaces in the rehabilitation of stroke and neurotrauma," *Systems Neuroscience and Rehabilitation*, K. Kansaku, L.G., Cohen, Eds. Berlin, Germany: Springer, 2011, pp. 3–18.

[9] S. R. Soekadar, M. Witkowski, N. Vitiello, and N. Birbaumer, "An EEG/EOG-based hybrid brain-neural computer interaction (BNCI) system to control an exoskeleton for the paralyzed hand," *Biomed. Eng.*, vol. 60, no. 3, pp. 199–205, Jun. 2015, doi: 10.1515/BMT-2014-0126.

[10] M. Witkowski, M. Cortese, M. Cempini, J. Mellinger, N. Vitiello, and S. R. Soekadar, "Enhancing brain-machine interface (BMI) control of a hand exoskeleton using electrooculography (EOG)," *J. Neuroeng. Rehabil.*, vol. 11, no. 1, Dec. 2014, Art. no. 165, doi: 10.1186/1743-0003-11-165.

[11] S. R. Soekadar, M. Witkowski, J. Mellinger, A. Ramos, N. Birbaumer, and L. G. Cohen, "ERD-based online brain-machine interfaces (BMI) in the context of neurorehabilitation: optimizing BMI learning and performance," *IEEE Trans. Neural Syst. Rehabil. Eng.*, vol. 19, no. 5, pp. 542–549, Oct. 2011.

[12] J. G. Colebatch and S. C. Gandevia, "The distribution of muscular weakness in upper motor neuron lesions affecting the arm," *Brain*, vol. 112, pp. 749–763, Jun. 1989, doi: 10.1093/BRAIN/112.3.749.

[13] L. M. Pain, R. Baker, D. Richardson, and A. M. Agur, "Effect of trunk-restraint training on function and compensatory trunk, shoulder and elbow patterns during post-stroke reach: A systematic review," *Disability Rehabil.*, vol. 37, no. 7, pp. 553–562, 2015, doi: 10.3109/09638288.2014.932450.

[14] S. Crea *et al.*, "Feasibility and safety of shared EEG/EOG and vision-guided autonomous whole-arm exoskeleton control to perform activities of daily living," *Sci. Rep.*, vol. 8, no. 1, Jul. 2018, Art. no. 10823, doi: 10.1038/s41598-018-29091-5.

[15] S. R. Soekadar *et al.*, "Restoration of finger and arm movements using hybrid brain/neural assistive technology in everyday life environments," in *Brain-Computer Interface Research, A State-of-the-Art Summary 7*, N. M.-K. Christoph Guger, B. Z. Allison, Eds. Berlin, Germany: Springer, 2019, ch. 5, pp. 53–61.

[16] E. Trigili *et al.*, "Design and experimental characterization of a shoulder-elbow exoskeleton with compliant joints for post-stroke rehabilitation," *IEEE/ASME Trans. Mechatronics*, vol. 24, no. 4, pp. 1485–1496, Aug. 2019.

[17] J. A. Diez, A. Blanco, J. M. Catalán, F. J. Badesa, L. D. Lledó, and N. Garcia-Aracil, "Hand exoskeleton for rehabilitation therapies with integrated optical force sensor," *Adv. Mech. Eng.*, vol. 10, no. 2, pp. 1–11, 2018.

[18] G. Ercolini, E. Trigili, A. Baldoni, S. Crea, and N. Vitiello, "A novel generation of ergonomic upper-limb wearable robots: Design challenges and solutions," *Robotica*, vol. 37, no. 12, pp. 2056–2072, Aug. 2019.

[19] S. Toyama, K. Takano, and K. Kansaku, "A non-adhesive solid-gel electrode for a non-invasive brain-machine interface," *Frontiers Neurol.*, vol. 3, no. 114, Jul. 2012, pp. 1–8, doi: 10.3389/FNEUR.2012.00114.

[20] G. Schalk, D. J. McFarland, T. Hinterberger, N. Birbaumer, and J. R. Wolpaw, "BCI2000: A general-purpose brain-computer interface (BCI) system," *IEEE Trans Biomed. Eng.*, vol. 51, no. 6, pp. 1034–1043, Jun. 2004.

[21] D. J. McFarland, "The advantages of the surface Laplacian in brain-computer interface research," *Int. J. Psychophysiol.*, vol. 97, no. 3, pp. 271–276, Sep. 2015, doi: 10.1016/J.IJPSYCHO.2014.07.009.

[22] G. Pfurtscheller and F. H. Lopes da Silva, "Event-related EEG/MEG synchronization and desynchronization: Basic principles," *Clin. Neurophysiol.*, vol. 110, no. 11, pp. 1842–1857, Nov. 1999, doi: 10.1016/S1388-2457(99)00141-8.

[23] C. Lauretti *et al.*, "Learning by demonstration for motion planning of upper-limb exoskeletons," *Frontiers Neurorobot.*, vol. 12, 2018, pp. 1–14, doi: 10.3389/FNBOT.2018.00005.

[24] A. J. Ijspeert, J. Nakanishi, H. Hoffmann, P. Pastor, and S. Schaal, "Dynamical movement primitives: Learning attractor models for motor behaviors," *Neural Comput.*, vol. 25, no. 2, pp. 328–373, 2013.

[25] M. I. Lourakis, "A brief description of the Levenberg-Marquardt algorithm implemented by levmar," *Found. Res. Technol.*, vol. 4, no. 1, pp. 1–6, 2005.

[26] C. D. Wolfe *et al.*, "Estimates of outcomes up to ten years after stroke: Analysis from the prospective South London Stroke Register," *PLoS Med.*, vol. 8, no. 5, May 2011, Art. no. e1001033, doi: 10.1371/JOURNAL.PMED.1001033.

[27] T. Ullberg, E. Zia, J. Petersson, and B. Norrving, "Changes in functional outcome over the first year after stroke: An observational study from the Swedish stroke register," *Stroke*, vol. 46, no. 2, pp. 389–394, Feb. 2015, doi: 10.1161/STROKEAHA.114.006538.

[28] W. Penfield and E. Boldrey, "Somatic motor and sensory representation in the cerebral cortex of man as studied by electrical stimulation," *Brain*, vol. 60, no. 4, pp. 389–443, 1937.

[29] M. H. Schieber, "Constraints on somatotopic organization in the primary motor cortex," *J. Neurophysiol.*, vol. 86, no. 5, pp. 2125–2143, 2001.

[30] A. Stancak, Jr., B. Feige, C. H. Lucking, and R. Kristeva-Feige, "Oscillatory cortical activity and movement-related potentials in proximal and distal movements," *Clin. Neurophysiol.*, vol. 111, no. 4, pp. 636–650, Apr. 2000, doi: 10.1016/s1388-2457(99)00310-7.

[31] S. R. Soekadar, N. Birbaumer, M. W. Slutzky, and L. G. Cohen, "Brain-machine interfaces in neurorehabilitation of stroke," *Neurobiol. Disease*, vol. 83, pp. 172–179, Nov. 2015, doi: 10.1016/j.nbd.2014.11.025.

[32] J. Ushiba and S. R. Soekadar, “Brain-machine interfaces for rehabilitation of poststroke hemiplegia,” *Prog. Brain Res.*, vol. 228, pp. 163–183, 2016, doi: 10.1016/bs.pbr.2016.04.020.

[33] J. Clausen *et al.*, “Help, hope, and hype: Ethical dimensions of neuroprosthetics,” *Science*, vol. 356, no. 6345, pp. 1338–1339, Jun. 2017, doi: 10.1126/science.aam7731.

[34] J. Iivanainen, M. Stenroos, and L. Parkkonen, “Measuring MEG closer to the brain: Performance of on-scalp sensor arrays,” *NeuroImage*, vol. 147, pp. 542–553, Feb. 2017, doi: 10.1016/j.neuroimage.2016.12.048.

[35] E. Boto *et al.*, “Moving magnetoencephalography towards real-world applications with a wearable system,” *Nature*, vol. 555, no. 7698, pp. 657–661, Mar. 2018, doi: 10.1038/nature26147.

[36] M. A. Cervera *et al.*, “Brain-computer interfaces for post-stroke motor rehabilitation: A meta-analysis,” *Ann. Clin. Translational Neurol.*, vol. 5, no. 5, pp. 651–663, May 2018, doi: 10.1002/acn3.544.

[37] A. Cavallo *et al.*, “Minimizing bio-signal recording sites for noninvasive hybrid brain/neural control,” *IEEE Syst. J.*, vol. 15, no. 2, pp. 1540–1546, Jun. 2021.

[38] L. N. Awad *et al.*, “A soft robotic exosuit improves walking in patients after stroke,” *Sci. Translational Med.*, vol. 9, no. 400, Jul. 2017, pp. 2182–2197, doi: 10.1126/scitranslmed.aai9084.

[39] M. Coscia *et al.*, “Neurotechnology-aided interventions for upper limb motor rehabilitation in severe chronic stroke,” *Brain*, vol. 142, no. 8, pp. 2182–2197, Aug. 2019, doi: 10.1093/brain/awz181.

[40] S. Hazubski, S. R. Soekadar, H. Hoppe, and A. Otte, “Neuroprosthetics 2.0,” *EBioMed*, vol. 48, Oct. 2019, Art. no. 22, doi: 10.1016/j.ebiom.2019.09.036.